

## Polymer-tool friction coefficient in temperature for thermoforming numerical simulation

CAUBET Benoit<sup>1,2,a \*</sup>, LÉONARDI Frederic<sup>2,b</sup> and AMAND Sylvain<sup>1,c</sup>

<sup>1</sup>University of Pau, Institut des Sciences Analytiques et de Physico-Chimie pour l'Environnement et les Matériaux, UMR 5254, 2 Av. Du Président Pierre Angot, 64000 Pau, FRANCE

<sup>2</sup>AXYAL, Aéroport Pyrénées, Rue de Bruscos, 64230 Sauvagnon, FRANCE

<sup>a</sup>benoit.caubet@univ-pau.fr, <sup>b</sup>frederic.leonardi@univ-pau.fr, <sup>c</sup>sylvain.amand@axyal.fr

**Keywords:** Thermoforming, Friction Coefficient, Numerical Simulation, Thickness Distribution, T-SIM®, Polycarbonate

**Abstract.** In this work, friction coefficient between Polycarbonate and Aluminum was measured over the entire thermoforming temperature range by using a rotational rheometer with a specific geometry, following the B. Hegemann *et al.* [1] method. The effects of velocity, pressure and surface roughness were investigated. Then, numerical simulation were performed using a finite element code package for thermoforming (T-SIM®) with K-BKZ viscoelastic model. The objective of this work is to find which friction coefficient use in T-SIM simulation to be as close as possible to reality. For this, numerical simulation results for different friction coefficient were compared with experimental values to evaluate the predictive capacity. It was shown that friction coefficient is temperature dependent and rapidly increase above glass transition of polycarbonate. At room temperature, friction coefficient increases with an increase in roughness, but after glass transition, trend is reversed. Simulations with measured friction coefficients shows good agreement with experiment data.

### Introduction

Thermoforming is a manufacturing process widely used in the industry for making 3D complex parts. An extruded polymer sheet is heated to be easily deformable and then vacuum formed on a cold mold. Despite the apparent simplicity of this process, it is actually a technical process, difficult to optimize, in which the material undergoes very large deformations in an anisotherm environment. Uneven thickness distribution is caused by localized variable deformations during vacuum forming. However, for manufacturers, a uniform thickness distribution and a high average thickness are very important parameters for the manufacture of high-quality parts. This thickness distribution is mainly affected by the viscoelastic behavior of the extruded polymer sheet [2,3,4] but previous work show that contact friction also has a huge impact on thickness distribution [2,5-8]. In the literature, the majority of authors study the effect of friction in the context of plug assist thermoforming. In this work, we will focus on conventional thermoforming, where the slip rate between the polymer and the mold is lower. Some studies claim that the friction coefficient does not depend on the sliding speed [1,5] but others show the opposite [9]. Several friction models exist but in this study we consider that the friction behavior between mold and polymer sheet can be simply represented using Coulomb friction law. This law defines friction coefficient as the ratio between the friction force and the normal force (Eq. 1):

$$\mu = \frac{F}{F_N} \quad (1)$$

Two friction coefficients can be defined : a static coefficient which corresponds to the minimum tangential force necessary to prime the slide and a dynamic coefficient which corresponds to the

tangential force necessary to maintain this slide. In this study, only the dynamic coefficient will be taken into account. The purpose of this work is to measure the impact of different parameters on the coefficient of friction between polycarbonate sheet and aluminum mold. The effects of velocity, pressure and surface roughness were investigated using a rotational rheometer with a specific geometry, following the method developed by B. Hegemann *et al* [1]. Measured friction values will be used in a numerical simulation of the thermoforming process and simulation results were compared with experimental data to evaluate the predictive capacity.

## Materials and Methods

Polycarbonate is a technical polymer with excellent mechanical properties and good temperature resistance. It is easily thermoformable thanks to its good flow resistance and is used in many fields such as automotive, aeronautic or medical. For this study a commercial polycarbonate LEXAN 9030 from SABIC was used. The initial sheet thickness was  $2,94 \pm 0,05$  mm. Temperature shrinkage is negligible ( $< 2\%$ ) in the extrusion or transverse direction. The glass transition temperature measured by DSC (rate:  $10^\circ\text{C}/\text{mn}$ ) is around  $T_g = 149^\circ\text{C}$ . Thermoforming molds and friction coefficient samples used for this study were made with Aluminum 5083 (AW-Al Mg4,5Mn0,7). Aluminum 5083 is a common aluminum-magnesium alloy with 4,5% magnesium.

### Torsional Rheometer Test Method.

The friction coefficient measuring device used in this study is based on the B. Hegemann *et al.* [1] method. developed at the IPK-Stuttgart. An Anton Paar MCR302 rotational rheometer is used in parallel configuration. The upper moving plate is replaced by the mold material sample and the polymer is fixed on the bottom. The test arrangement is shown in Fig. 1a. After contact, the torque required to rotate both parts is measured and converted into a coefficient of friction. Applied normal force and rotation speed are easily adjustable over a wide range of values representative of the thermoforming process. The device is placed in a temperature-regulated chamber, suitable for making measurements from room temperature until forming temperature. Between each measurement, the upper plate is cleaned with acetone to remove any residual traces of polymer. In order to reproduce as much as possible a linear sliding during the test and minimize the velocity gradient, the contact surface is limited to one ring (Fig. 1b). Inner and outer radii are respectively 9 mm and 12.5 mm. As a result, the maximum speed rotation varies only about 15% around the mean value. The tested polymer sample is a 25 mm disc, glued on a disposable plate with a two-component epoxy adhesive resistant up to  $180^\circ\text{C}$ . Special attention is paid to the flatness of the experimental setup to ensure optimal contact.

Thus, assuming that the normal force is evenly distributed over the contact surface, and taking into account the geometry used, the average friction coefficient can be calculated from the following relation [Eq. 2] :

$$\mu = \frac{3}{2} \times \frac{\tau}{F_N} \times \frac{R_o^2 - R_i^2}{R_o^3 - R_i^3} \quad (2)$$

where  $\Gamma$  is the measured torque,  $F_N$  the normal force and  $R_i$  and  $R_o$  are respectively the inner and outer radius of the ring.

### Test settings.

With this method, friction coefficients were measured over a wide range of temperature, from room temperature to  $180^\circ\text{C}$ . First every  $40^\circ\text{C}$  up to  $140^\circ\text{C}$ , then, every  $10^\circ\text{C}$  from the glass transition temperature of polycarbonate samples ( $T_g = 149^\circ\text{C}$ ). Beyond  $180^\circ\text{C}$ , the epoxy adhesive fail and does not maintain the sample properly. This temperature range does not cover the entire forming range (up to  $220^\circ\text{C}$  for polycarbonate) but in reality, due to the low thermal effusivity of polycarbonate compared to aluminium, interface temperature is much lower and probably no more than  $180^\circ\text{C}$ . Some previous studies [1, 9] show that there is no significant influence of normal

force on friction coefficient. In order to verify this hypothesis, friction coefficients were measured at room temperature for several values of normal force (2, 5 and 10N). For higher temperatures, the normal force was limited to 2N because of MCR302 torque measurement limitation but also to limit compression deformations beyond glass transition temperature.

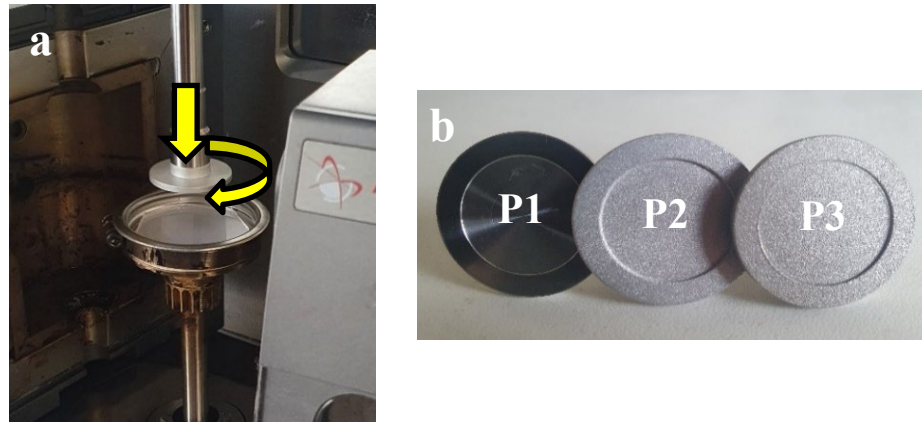


*Fig. 1. (a) Modified rotational rheometer with aluminum upper plate and polymer sample on the lower plate. (b) P1, P2 and P3 aluminum plate with roughness of respectively  $R_a = 0,38 \mu\text{m}$ ,  $R_a = 2,80 \mu\text{m}$  and  $R_a = 8,12 \mu\text{m}$ . Contact surface is limited to a crown of 9 mm inner radius and 12.5 mm outer radius.*

In order to measure the impact of the sliding speed on the friction coefficient, different rotational speeds were investigated. In industry, the mold rising speed is typically within the range 25-100 mm/s. However, glide speed can be considerably less due to the frictional force and the sheet deformation resistance [5, 9]. Thus, for the sake of covering a representative sliding speeds range of the thermoforming process, friction coefficients were measured for three different rotational speeds of 4.4 rpm, 11.1 rpm and 22.2 rpm corresponding respectively to an average sliding speed of 5 mm/s, 12.5 mm/s and 25 mm/s. In addition, all these measurements were carried out for three different aluminium upper plates surface roughness, corresponding to different surface states of industrial moulds (Fig. 1b). The plate 1 (P1) corresponds to a smooth mold with  $R_a = 0,38 \mu\text{m}$  while plate 2 (P2) and 3 (P3) have been sanded with roughnesses of  $R_a = 2,80 \mu\text{m}$  and  $R_a = 8,12 \mu\text{m}$  respectively. The various tested parameters are summarized in Table 1. This experimental design allows the coverage of a wide range of friction coefficients values on all the thermoforming process parameter range.

### Friction Measurement Results and Discussions

Fig. 2 shows the evolution of the coefficient of friction at room temperature as a function of the normal force for applied values of 2 N, 5 N, and 10 N. For the P1 plate with the smoothest surface, normal force does not affect the friction coefficient in the measurement range. For P2 and P3 plates, with a rougher surface, the friction coefficient increases slightly with normal force. Increase in the normal force must increase the penetration of the roughnesses into the polymer and therefore the friction.

*Table 1. Friction coefficient measurement parameters.*

	Roughness ( $\mu\text{m}$ )	Temperature range ( $^{\circ}\text{C}$ )	Normal Force (N)	Rotation speed (mm/s)
Plate 1 (P1)	0,38	20	2 - 5 - 10	5 - 12,5 - 25
		60-180	2	
Plate 2 (P2)	2,80	20	2 - 5 - 10	5 - 12,5 - 25
		60-180	2	
Plate 3 (P3)	8,12	20	2 - 5 - 10	5 - 12,5 - 25
		60-180	2	

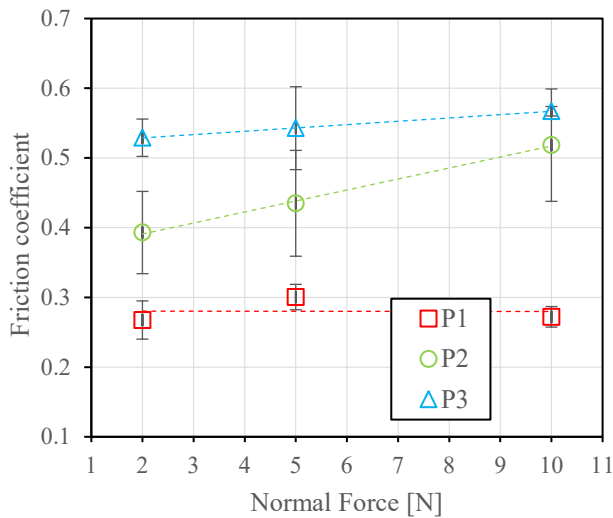


Fig. 2. Friction coefficient at room temperature for an applied normal force of 2N, 5N and 10N (Speed test = 12,5mm/sec).

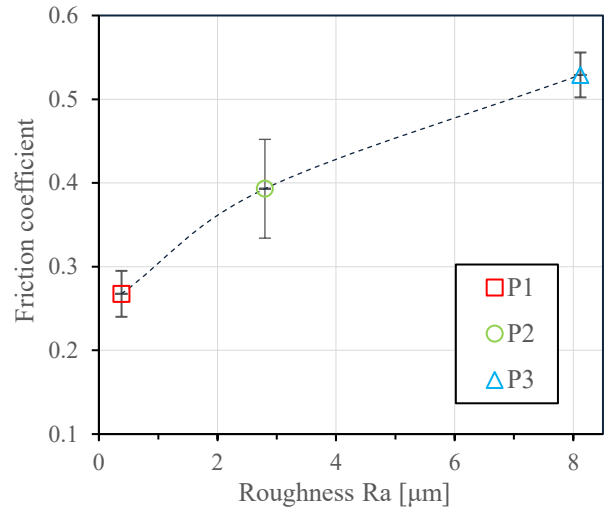


Fig. 3. Friction coefficient in function of roughness (Normal force = 2N, Speed test = 12,5 mm/sec).

Friction coefficient evolution with surface roughness at room temperature is reported in Fig. 3. Contrary to expectation the coefficient of friction increases with the surface roughness by almost following a linear relationship. This result contradicts previous studies [10, 11] assuming that the apparent surface contact reduction due to the roughness decreased friction. One possible explanation is that, in reality, the friction force can be divided into two independent contributions: an adhesive term representing the adhesion phenomena at the real contact level and a deformation term representing volumic deformations by “ploughing”. This deformation term is sometimes not negligible at room temperature [12]. It is possible that in the case of the roughness profile of the P2 and P3 plates, the deformation term is important and increases the friction coefficient.

In temperature, for a 2N applied force, Fig. 4 shows that the friction coefficient is stable up to the glassy transition temperature (~150°C) and then increases more or less significantly with roughness. This results is consistent with literature [1, 2, 9]. However, there is a

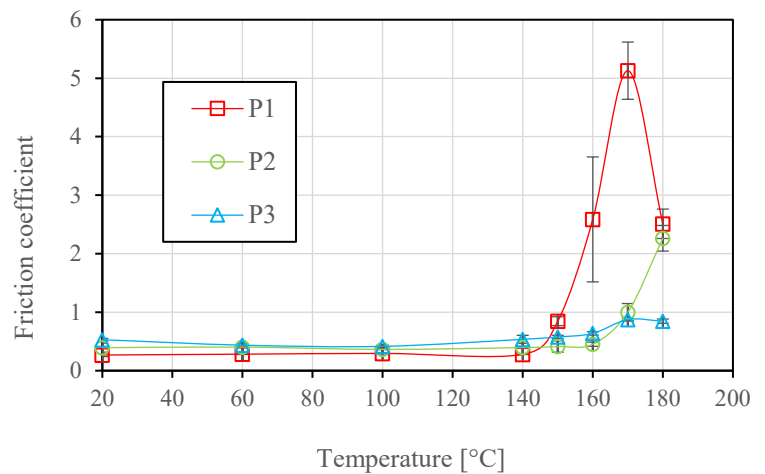


Fig. 4. Effect of temperature on friction coefficient for the three plates (Normal force = 2N, Speed test = 12.5mm/sec).

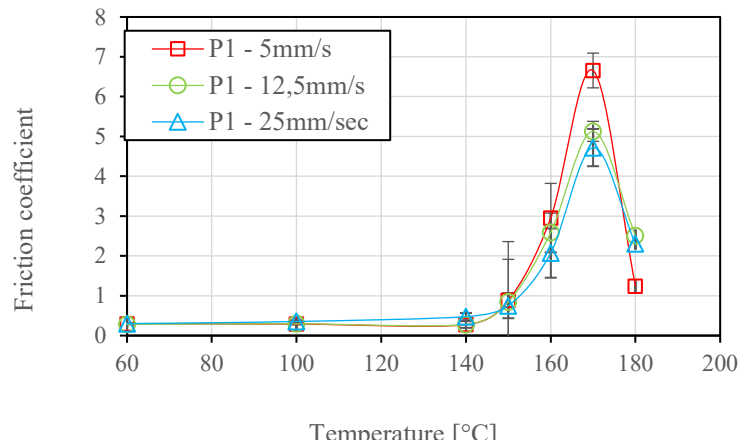


Fig. 5. Effect of speed sliding on friction coefficient in temperature for smooth plate P1 (Normal force = 2N).

decrease of friction coefficient in temperature as a function of the surface roughness. It is deduced that, unlike to ambient temperature, the drop in mechanical properties due to temperature increase reduces the deformation term effect on friction in favor of the adhesion term. Friction coefficient decline from 180°C can be explained by a totally sticky contact, the measured torque being linked to pure shear of the sample [1]. Fig. 5 shows the effect of the sliding speed on the friction coefficient for P1 plate. The decrease in the sliding speed increases friction. This sensitivity to speed and temperature relates the viscoelastic behavior of polymers and Time Temperature Superposition (TTS) principle. This behavior has already been observed in the case of elastomers [12] as well as on impact PS and PP [9]. The behavior is the same with the P2 and P3 plates.

### Numerical Simulation and Experimental Comparison

T-SIM software.

The 3D numerical simulations were carried out using the commercial package code T-SIM® version 4.9 (Accuform) based on the finite element method and specially designed for the simulation of the thermoforming process. This software use a K-BKZ [13] type nonlinear viscoelastic constitutive model to describe large polymer deformations during forming. Friction Coulomb's law was applied on contact areas between sheet and mold, and the heat equation allows the calculation of thermal transfers during the process. The thickness distribution and polymer stretching were numerically investigated for the different experimentally measured friction coefficient values. Next, numerical results were compared with experimental thermoforming data obtained with two representative moulds presented in Fig. 8. The mold A has the same surface roughness as plate P1 ( $R_a = 0,41 \mu\text{m}$ ) and the mold B has the same as plate P3 ( $R_a = 8,06 \mu\text{m}$ ).

Viscoelastic model parameters.

During thermoforming, polymer materials exhibit nonlinear viscoelastic behavior due to large deformations and high strain rates over a wide range of temperatures. To describe this particular behavior, T-SIM use the K-BKZ type viscoelastic Wagner Model. This model shows good results for the simulation of the thermoforming process for ABS [2, 4], PS [14], or HDPE [15]. The Wagner model is expressed as follows (3):

$$\sigma(t) = \int_{-\infty}^t m(t - t')h(I_1, I_2)C^{-1}(t, t') \quad (3)$$

- $C^{-1}(t, t')$  is the finger strain tensor.  $I_1$  and  $I_2$  are invariants and depend on the solicitation type.
- $m(t - t')$  is the time dependent Memory function used to explain the linear viscoelasticity. The memory function is calculated from the discrete relaxation spectra obtained by small amplitude oscillatory shear (SAOS) experiment. Several experiments were carried out at different temperatures and the master curve was reconstructed thanks to the time-temperature equivalence principle and the Williams-Landel-Ferry (WLF) equation.
- $h(I_1, I_2)$  is the Damping of the two strain invariants used to describe the nonlinear viscoelasticity. T-SIM software uses the following damping function Wagner (4) :

$$h(I_1, I_2) = \frac{1}{1 + A\sqrt{(I_1-3)(I_2-3)}} \quad (4)$$

K-BKZ Wagner damping function was numerically determined using T-SIMFIT® v1.41 software from uniaxial tensile test data. Tensile test were carried out at 170, 180 and 190°C and for four different speeds of 1.25, 2.5 and 12.5 mm/sec corresponding to an initial elongation rate

of 0.1, 0.5 and 1 s<sup>-1</sup> respectively. Fig. 6 shows the prediction from Wagner model for  $A = 0,095$  in comparison with experimental data at 170°C.

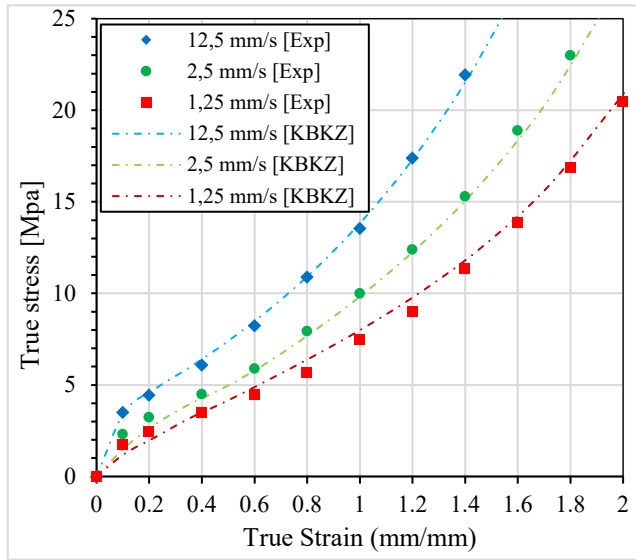


Fig. 6. Lexan 9030 stress/strain curve at 170°C. Experimental data are represented by symbols and KBKZ prediction by dashed lines for  $A = 0,095$ .

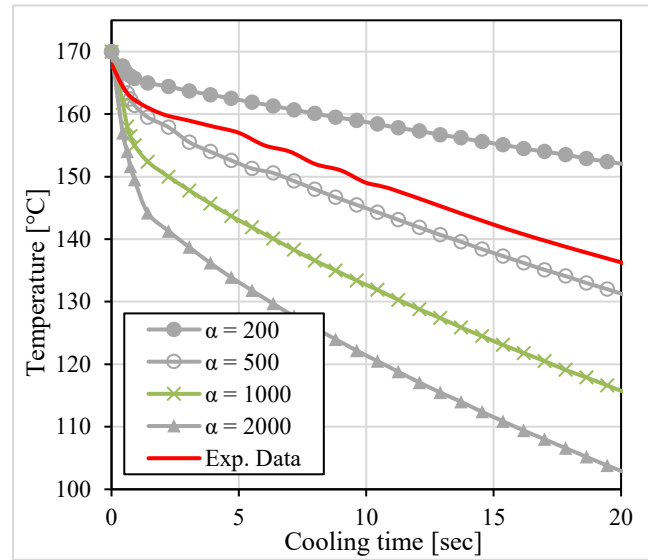


Fig. 7. Cooling of a Lexan 9030 sheet at 170°C during 20sec. Red line correspond to experimental cooling measured by thermal camera and gray lines are simulated cooling for different conductive exchange coefficient.

#### Heat transfer.

As shown above, the viscoelastic behaviour of polymers is highly temperature dependent. Therefore, it is necessary to well know the temperature throughout the forming cycle. For this purpose, a heat equation makes it possible to account for heat exchanges during the process. The polycarbonate thermal capacity and thermal conductivity were determined on a large temperature range by measurement in modulated DSC and HOT DISK device. The measured values are respectively  $C_p = 2.140 \text{ J/(Kg.K)}$  and  $\lambda = 0.22 \text{ W/(m.K)}$  at 180°C. In T-SIM, thermal properties are constant but in reality, they are temperature dependent, particularly around the  $T_g$ . For mold and sheet heat exchanges, the mold is only represented by its external surface and is assumed to be isothermal throughout the operation. The mold's thermal properties are not involved in it, and it is considered that the sheet-mold heat flow is monitored by a conductive exchange coefficient called " $\alpha$ ". It may not hold a tangible sense, but it may however be experimentally determined : the cooling of a Lexan 9030 sheet at a temperature of 170°C, in contact with an aluminum mold at room temperature could be measured and then compared to simulated cooling for different  $\alpha$  values (Fig 7). As a result, conductive exchange coefficients were found to be close to 500  $\text{W/m}^2/\text{K}$ , which is similar to a value obtained by Marotta and Fletcher [16]. Likewise, the convection exchange coefficient between polymer and ambient air is 8  $\text{W/m}^2/\text{K}$ .

#### Friction coefficient.

At the areas of contact between sheet and mold, sliding is managed by the Coulomb friction law. As with thermal properties, the friction coefficient is considered constant throughout the forming cycle. This study showed that in reality, the friction coefficient depends on several parameters and is largely temperature dependent for polymers. Several friction coefficients corresponding to the previously measured coefficients have been tested and the simulation will be compared with the experimental results.

Process parameters.

T-SIM software makes it possible to easily manage the various process parameters to best match the experimental parameters (see *Experimental thermoforming*). The initial sheet temperature is 215°C. The mold rising speeds are respectively 20 cm/s and 10 cm/s for mold A and mold B. No pre-stretching were performed and a vacuum of - 0.2 bar is applied for 5s. A 60,000 polygons mesh permit to have an optimal compromise between precision and calculation time. Different process parameters are summarized in Table 2.

Experimental thermoforming.

Experimental thermoforming was performed on a laboratory scale thermoforming machine Formech 450DT. A thermal camera placed above the device allows sheet temperature profile recording in real time. The pressure during the forming cycle is measured by a manometer. Fig. 9 shows the experimental setup. The polymer sheet is heated with ceramic radiants until reaching a temperature of 215°C. In order to achieve the most uniform temperature distribution possible, the power of the external radiants is slightly increased to compensate heat losses by convection with ambient air. The rise of the mold is manually controlled. The average mold speed is around 20 cm/sec for mold A and 10 cm/sec for mold B, in order to avoid tearing the sheet on sharp angle. Then, a vacuum of -0.2 bar is applied for 5 to 7 sec to form the sheet on the mold.

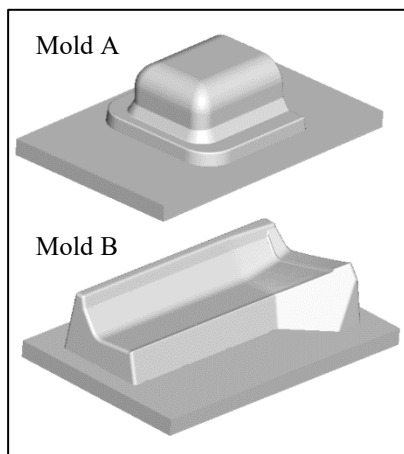


Fig. 8. Molds used for experimental thermoforming and simulation. Mold A has a surface rugosity of  $R = 0,41 \mu\text{m}$  corresponding to plate P1 and Mold B,  $R_a = 8,06 \mu\text{m}$  corresponding to plate P3.



Fig. 9. Experimental thermoforming setup with Formech 450DT thermoforming machine and thermal camera.

Table 2. Process parameter for numerical simulation with T-SIM®.

Process parameters	Mold roughness	Mold temp.	Sheet temp.	Mold speed	Convection coefficient	Conduction coefficient	Vacuum pressure
Mold A	0,41 $\mu\text{m}$	70°C	215°C	20 cm/s	8	500	0,2 bar during 5 sec
Mold B	8,06 $\mu\text{m}$	95°C		10 cm/s			

### Simulation and Experimental Comparison Results

Several simulations were carried out with process parameters presented in Table 2. Four coefficients of friction were simulated as a function of the two molds:  $\mu = 0.3$  (minimum coefficient of friction for the polycarbonate-plate couple P1),  $\mu = 0.75$ ,  $\mu = 1.5$  and  $\mu = 5$  (corresponding to total stick) for the mold A and  $\mu = 0.5$  (minimum friction coefficient for



polycarbonate-plate P3)  $\mu = 0.75$ ,  $\mu = 1.5$  and  $\mu = 5$  for mold B. For each mold and friction coefficient, the simulated thickness distribution along the transverse (A-A) and longitudinal (B-B) axis is represented by a continuous line in Fig. 10 and Fig. 11. Experimental thicknesses has been measured on at least two different thermoformed parts using a digital micrometer is represented by diamond symbols. The thickness distribution can be divided in two regions: the upper part and the side parts. For mold A, uppers parts are located from 150 mm to 250 mm for transversal cut and from 225 mm to 375 mm for longitudinal cut. For mold B, uppers parts are located from 150 mm to 275 mm for transversal cut and from 75 mm to 425 mm for longitudinal cut. Other parts are considered as side parts.

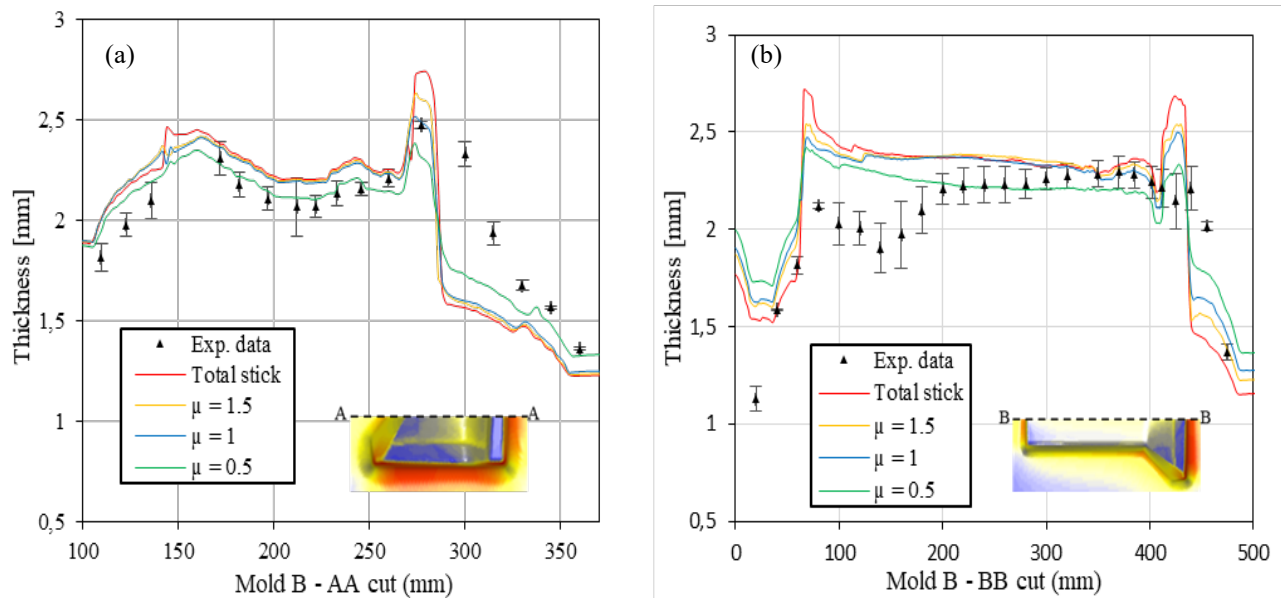


Fig. 11. Mold B thickness distribution along transversal (A-A) axis (a) and longitudinal (B-B) axis (b). Simulated data are in continuous line and experimental data are represented by diamond symbols.

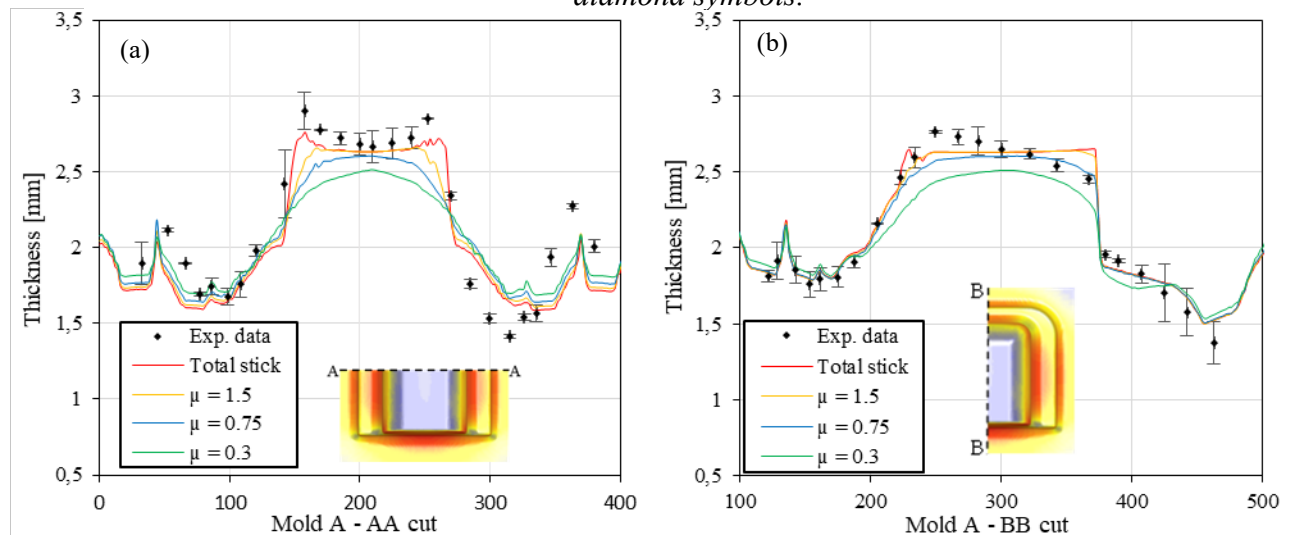


Fig. 10. Mold A thickness distribution along transversal (A-A) axis (a) and longitudinal (B-B) axis (b). Simulated data are in continuous line and experimental data are represented by diamond symbols.

The effect of friction coefficient variation is particularly visible on mold upper parts, the first in contact with polymer sheet during forming. The higher the friction coefficient, the greater the



simulated thickness. Indeed, when the friction coefficient is important or when the contact is completely sticky, the sheet cannot slide on the surface of the mold. Thus, the deformations are mainly concentrated on the side parts and in the corners. This phenomenon is amplified by the sheet cooling in contact with mold, which limits the polymer's ability to deform under stress. We can deduce from its results that a lower friction coefficient promotes a more uniform thickness distribution especially when the mold geometry has a large upper planar surface.

Overall, for the two molds, simulated thickness distribution shows good agreement with experimental data. For mold A [Fig. 10a and 10b], average measured thickness on the upper part corresponds to simulated thickness for high friction coefficient, see even, for total stick behavior on [Fig. 10a].

Its results confirm the friction coefficients measured previously: since the polymer sheet is still close to 215°C when in contact with the mold, P1 plate friction coefficient measurements predict sticky contact for this temperature. For mold B [Fig. 11a and 11b], average measured thickness on the upper part gets closer to simulated thickness for a friction coefficient between  $\mu = 0.5$  and 1. Again, this corresponds to friction coefficient value measured for plate P3 at this temperature. Based on these results, the sanding of the thermoforming tools makes it possible to limit the friction with sheet polymer in temperature and thus greatly improve the average thickness distribution.

### Summary

A rotational rheometer with a specific geometry allowed us to measure the coefficient of friction from the ambient temperature up to the forming temperature for different speeds of rotation and normal force. Effect of surface roughness was explored. It was shown that friction coefficient is temperature dependent and rapidly increases above glass transition. At room temperature, contrary to expectation, friction coefficient increases with an increase in roughness. One possible explanation is that, for this couple of materials, the friction deformation term is not negligible at room temperature and results in an increase of friction for rough plate. After glass transition, this trend is reversed and the smooth plate (P1) exhibits sticky behavior beyond 180°C. Simulations with T-SIM<sup>®</sup> show good agreement with experimental data and confirm the friction coefficient values in temperature for the different roughnesses. For mold A (smooth surface corresponding to plate P1), best match is reached for a very high friction coefficient. For sand mold B (corresponding to plate P3), friction coefficients between 0.5 and 1 show best results. Based on these results, the sanding of the thermoforming tools makes it possible to limit the friction with sheet polymer in temperature and thus greatly improve the average thickness distribution.

### Acknowledgments

This work was supported by ANRT funding and AXYAL (Sauvagnon, FRANCE) as part of a CIFRE PhD thesis.

### References

- [1] Information on: Polymer\_Polymeric\_Hegemann2003\_(methode par rhéo).pdf
- [2] J.K. Lee, C.E. Scott, T.L. Virkler, Effects of rheological properties and processing parameters on ABS thermoforming, *Polym. Eng. Sci.* 41 (2001) 240-261. <https://doi.org/10.1002/pen.10725>
- [3] M. Takaffoli, G. Hangalur, R. Bakker, N. Chandrashekar, Thermo-visco-hyperelastic behavior of polycarbonate in forming of a complex geometry, *J. Manuf. Process.* 57 (2020) 105-113. <https://doi.org/10.1016/j.jmapro.2020.06.019>
- [4] J. Cha, H.Y. Song, K. Hyun, J.S. Go, Rheological measurement of the nonlinear viscoelasticity of the ABS polymer and numerical simulation of thermoforming process, *Int. J. Adv. Manuf. Technol.* 107 (2020) 2449-2464. <https://doi.org/10.1007/s00170-020-04979-7>
- [5] P.J. Martin, R. McCool, C. Härter, H.L. Choo, Measurement of polymer-to-polymer contact friction in thermoforming, *Polym. Eng. Sci.* 52 (2012) 489-498. <https://doi.org/10.1002/pen.22108>

- [6] D. Marathe, D. Rokade, L. Busher Azad, K. Jadhav, S. Mahajan, Z. Ahmad, S. Gupta, S. Kulkarni, V. Juvekar, A. Lele, Effect of Plug Temperature on the Strain and Thickness Distribution of Components Made by Plug Assist Thermoforming, *Int. Polym. Process.* 31 (2016) 166-178. <https://doi.org/10.3139/217.3060>
- [7] R.A. Morales, M.V. Candal, O.O. Santana, A. Gordillo, R. Salazar, Effect of the thermoforming process variables on the sheet friction coefficient, *Mater. Des.* 53 (2014) 1097-1103. <https://doi.org/10.1016/j.matdes.2013.08.009>
- [8] P. Collins, E.M.A. Harkin-Jones, P.J. Martin, The Role of Tool/Sheet Contact in Plug-assisted Thermoforming, *Int. Polym. Process.* 17 (2002) 361-369. <https://doi.org/10.3139/217.1702>
- [9] A. Erner, Étude expérimentale du thermoformage assisté par poinçon d'un mélange de polystyrènes, p. 232.
- [10] J. Voyer, S. Klien, I. Velkavrh, F. Ausserer, A. Diem, Static and Dynamic Friction of Pure and Friction-Modified PA6 Polymers in Contact with Steel Surfaces: Influence of Surface Roughness and Environmental Conditions, *Lubricants* 7 (2019) 17. <https://doi.org/10.3390/lubricants7020017>
- [11] V. Quaglioni, P. Dubini, D. Ferroni, C. Poggi, Influence of counterface roughness on friction properties of engineering plastics for bearing applications, *Mater. Des.* 30 (2009) 1650-1658. <https://doi.org/10.1016/j.matdes.2008.07.025>
- [12] B. Briscoe, The friction of polymers : a short review, *Proc. 7 th Leeds-Lyon Symposium of tribology*, N° 00682, 1980, pp. 9-1281.
- [13] E. Mitsoulis, 50 Years of the K-BKZ Constitutive Relation for Polymers, *ISRN Polym. Sci.* 2013 (2013) 1-22. <https://doi.org/10.1155/2013/952379>
- [14] K. Landsecker, C. Bonten, Thermoforming simulation of heat conductive plastic materials using the K-BKZ model, presented at the Materials characterization using X-rays and related techniques, Kelantan, Malaysia, 2019, p. 030049. <https://doi.org/10.1063/1.5088307>
- [15] S. aus der Wiesche, Industrial thermoforming simulation of automotive fuel tanks, *Appl. Therm. Eng.* 24 (2004) 2391-2409. <https://doi.org/10.1016/j.applthermaleng.2004.03.003>
- [16] E.E. Marotta, L.S. Fletcher, Thermal contact conductance of selected polymeric materials, *J. Thermophys. Heat Trans.* 10 (1996) 334-342. <https://doi.org/10.2514/3.792>